

See discussions, stats, and author profiles for this publication at: <https://www.researchgate.net/publication/231680671>

# New Mesostructured Porous TiO<sub>2</sub> Surface Prepared Using a Two-Dimensional Array-Based Template of Silica Particles

ARTICLE *in* LANGMUIR · OCTOBER 1998

Impact Factor: 4.46 · DOI: 10.1021/la981106z

---

CITATIONS

117

---

READS

37

4 AUTHORS, INCLUDING:



**Tetsuya Miwa**

Japan Agency for Marine-Earth Science Tech...

52 PUBLICATIONS 1,189 CITATIONS

SEE PROFILE



**Donald A. Tryk**

University of Yamanashi

250 PUBLICATIONS 15,577 CITATIONS

SEE PROFILE

# New Mesostructured Porous TiO<sub>2</sub> Surface Prepared Using a Two-Dimensional Array-Based Template of Silica Particles

Sachiko I. Matsushita, Tetsuya Miwa, Donald A. Tryk, and Akira Fujishima\*

Department of Applied Chemistry, School of Engineering, The University of Tokyo,  
7-3-1 Hongo, Bunkyo-ku, Tokyo 113-8656, Japan

Received August 25, 1998

Mesoporous photocatalytic titanium dioxide films with periodic structures were prepared by molding from two-dimensionally ordered arrays of monodisperse SiO<sub>2</sub> particles. The morphology of the porous structures in these films was dependent upon the annealing temperature. The photocatalytic activity of the films was confirmed, as evidenced by the photodeposition of silver on the textured film surfaces. Attachment of the free-standing films to rigid supports allowed us to locate specific microscopic areas at will and to monitor the progress of the silver photodeposition in these areas using optical microscopy and scanning electron microscopy, with both secondary electron and backscattered electron detection. However, the repeated electron beam exposure in these selected areas was found to adversely affect the photoreducibility. Although the detailed film morphology did not affect the macroscopic photocatalytic activity, we found subtle differences in the silver nucleation process which depended upon the pore wall thickness.

## Introduction

Nanoporous semiconducting materials have recently attracted much attention because of their various applications in electronic, electrochemical, and photocatalytic systems, including photoelectrochemical solar cells,<sup>1–3</sup> electrocatalysts,<sup>4–6</sup> sensors,<sup>7</sup> and high-performance photocatalytic films.<sup>8</sup> Many efforts have been made to prepare nanoporous semiconducting materials with textured surfaces of controlled periodicity in order to optimize the mass transport properties.<sup>9–12</sup> For example, to prepare porous films for liquid junction solar cell applications or for faster gas diffusion in sensors, the widths of the hollow channels need to be on the order of tens or hundreds of nanometers,<sup>13</sup> that is, mesopores. Recent examples of the preparation of mesoporous TiO<sub>2</sub> materials include the use of emulsion templating<sup>11</sup> and replication of three-dimensional latex arrays, the latter produced via either filtration<sup>14</sup> or ultracentrifugation.<sup>15</sup>

We have recently reported the use of a new technique for the preparation of highly ordered mesoporous TiO<sub>2</sub> thin films using a two-dimensional (2D) array of monodisperse solid particles as a template.<sup>16</sup> This approach promises to provide a versatile means of producing thin

coatings (0.5–2 μm) with a range of pore dimensions (0.1–1.0 μm),<sup>17</sup> using 2D arrays of either silica<sup>16</sup> or latex spheres.<sup>18</sup> 2D arrays have been well-studied recently, in part because of the large range of particle sizes (tens of nanometers to several micrometers).<sup>19–25</sup> In such arrays, fine latex particles<sup>20,21</sup> or protein molecules<sup>22</sup> are packed in high-density, highly oriented layers over a wide surface area due to water evaporation and lateral capillary forces (also referred to as capillary immersion forces<sup>23</sup>). These arrays have been discussed in the literature from both the viewpoint of high-density optical storage media<sup>24,25</sup> and that of the orientation of protein molecules.<sup>22</sup>

In our preliminary report, we demonstrated the feasibility of fabricating porous TiO<sub>2</sub> films with highly ordered porosity by means of replication from 2D arrays of silica particles.<sup>16</sup> The mesopore morphology was found to change with the annealing temperature. In the present paper, we report on this technique in greater detail and focus on the photocatalytic properties, which we have examined using the photodeposition of silver particles from silver nitrate solution.<sup>26,27</sup> This approach enables us to confirm that the photoreduction process takes place on the mesostructured surface. It also enables us to examine in detail, at the submicrometer level, the relationships

- (1) Hagfeldt, A.; Grätzel, M. *Chem. Rev.* **1995**, *95*, 49.
- (2) Lindstrom, H.; Rensmo, H.; Sodergren, S.; Solbrand, A.; Lindquist, S. E. *J. Phys. Chem.* **1996**, *100*, 3084.
- (3) Boschloo, G. K.; Goossens, A. *J. Phys. Chem.* **1996**, *100*, 19489.
- (4) Hoyer, P. *Langmuir* **1996**, *14*, 1411.
- (5) Moriguchi, I.; Maeda, H.; Teraoka, Y.; Kagawa, S. *Chem. Mater.* **1997**, *9*, 1050.
- (6) Lakshmi, B. B.; Dorhout, P. K.; Martin, C. R. *Chem. Mater.* **1997**, *9*, 857.
- (7) Hoyer, P.; Masuda, H. *J. Mater. Sci. Lett.* **1996**, *15*, 1228.
- (8) Gopidas, K. R.; Bohorques, M.; Kamat, P. V. *J. Phys. Chem.* **1990**, *94*, 6435.
- (9) Masuda, H.; Nishio, K.; Baba, N. *Jpn. J. Appl. Phys.* **1992**, *31*, L1775.
- (10) Routkevitch, D.; Bigioni, T.; Moskovits, M.; Xu, J. M. *J. Phys. Chem.* **1996**, *100*, 14037.
- (11) Imhof, A.; Pine, D. J. *Nature* **1997**, *389*, 948.
- (12) Douglas, K.; Devaud, G.; Clark, N. A. *Science* **1992**, *257*, 642.
- (13) Konenkamp, R.; Henninger, R. *Appl. Phys. A* **1994**, *58*, 87.
- (14) Holland, B. T.; Blanford, C. F.; Stein, A. *Science* **1998**, *284*, 538.
- (15) Wijnhoven, J. E. G. J.; Vos, W. L. *Science* **1998**, *281*, 802.

- (16) Matsushita, S.; Miwa, T.; Fujishima, A. *Chem. Lett.* **1997**, 309, 925.
- (17) Matsushita, S. I.; Miwa, T.; Tryk, D. A.; Fujishima, A. In preparation.
- (18) Ikezawa, A.; Miwa, T.; Fujishima, A. In preparation.
- (19) Denkov, N. D.; Velev, O. D.; Kralchevsky, P. A.; Ivanov, I. B.; Yoshimura, H.; Nagayama, K. *Nature* **1993**, *361*, 26.
- (20) Yamaki, M.; Higo, J.; Nagayama, K. *Langmuir* **1995**, *11*, 2975.
- (21) Matsushita, S.; Miwa, T.; Fujishima, A. *Langmuir* **1997**, *13*, 2582.
- (22) Nagayama, K.; Takeda, S.; Endo, S.; Yoshimura, H. *Jpn. J. Appl. Phys.* **1995**, *34*, 3947.
- (23) Dushkin, C. D.; Kralchevsky, P. A.; Paunov, V. N.; Yoshimura, H.; Nagayama, K. *Langmuir* **1996**, *12*, 641.
- (24) Micheletto, R.; Fukuda, H.; Ohtsu, M. *Langmuir* **1995**, *11*, 3333.
- (25) Hayashi, S.; Kumamoto, Y.; Suzuki, T.; Hirai, T. *J. Colloid Interface Sci.* **1991**, *144*, 538.
- (26) Herrmann, J.-M.; Disdier, J.; Pichat, P. *J. Catal.* **1988**, *113*, 72.
- (27) Ohtani, B.; Nishimoto, S. *J. Phys. Chem.* **1993**, *97*, 920.

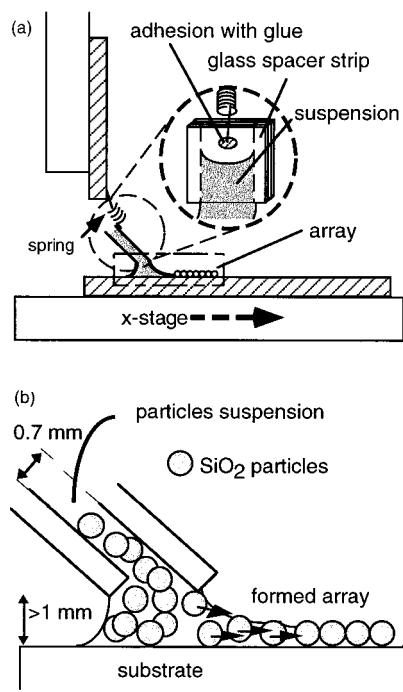


**Figure 1.** Schematic diagram of the cell used to fabricate the arrays. (a) The thickness of the array was controlled by adjusting the distance between the cell and the substrate using the  $z$ -axis stage. During preparation of the array, the substrate is translated horizontally using the  $x$ -axis stage. (b) Detail depicting the formation of the 2D array from the fine particles by lateral capillary force, corresponding to the dashed rectangle in part a.

between the film morphology and the photodeposition process, using scanning electron microscopy (SEM).<sup>28–30</sup> We have developed a technique for immobilizing the fragile free-standing films in an oriented fashion on a macroscopic support, so that it is possible to monitor the progress of the photodeposition with irradiation time in specific microscopic locations. We also examined differences in the Ag particle nucleation process for two different morphologies of pore structures and proposed a simple model to explain these differences.

### Materials and Methods

**Preparation: Silica 2D Array.** Monodisperse silica ( $\text{SiO}_2$ ) particles were used to prepare two-dimensional (2D) ordered arrays as replica templates. These particles are stable at  $\text{TiO}_2$  annealing temperatures (400–500 °C). Fine monodisperse microspherical  $\text{SiO}_2$  particles were obtained from Nippon Syokubai, Japan (Seahostar KE-P,  $530 \pm 50$  nm in diameter). The  $\text{SiO}_2$  particles were suspended (4.8 wt %) in 2-propanol. The  $\text{SiO}_2$  particle arrays were prepared on microscope cover glass sheets (Takahashi Giken Glass, Japan) from the suspension. The numbers of layers of particles in the arrays were controlled using methods reported previously.<sup>14</sup>

An apparatus for the preparation of the 2D arrays was constructed using a small glass cell (Figure 1). This cell, which was fabricated using cover glasses, was  $25 \times 25$  mm<sup>2</sup>, with a gap width of 0.7 mm. The spring acts as a device to mechanically decouple the  $z$ -axis stage from the cell and the 2D array. Approximately 0.5 mL of the suspension was injected into the cell. A glass support plate for the cell was attached vertically to a  $z$ -axis stage, and a glass substrate for the preparation of the 2D arrays was attached to an  $x$ -axis stage. The movement of

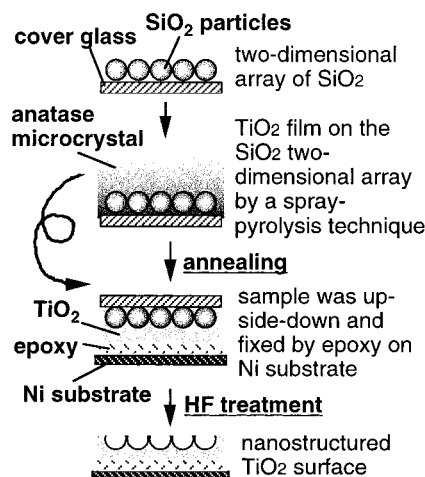


**Figure 2.** Schematic process for fabrication of mesoporous structured  $\text{TiO}_2$  films.

these stages can be controlled at rates from 0.1 to 300  $\mu\text{m/s}$ . The substrates were nonfluorescent glass slides ("Micro-Slide" glass, Matsunami, Co., Japan).

Initially, the lower edge of the cell was positioned to within 0.1 mm of the substrate using the  $z$ -axis stage. Then the suspension was injected, forming a meniscus, as shown in Figure 1b. Next, the substrate was translated several micrometers with the  $x$ -axis stage in order to form a broad-based meniscus. Then this stage was translated continuously at a controlled rate (see below). The coating of particles begins to form within the trailing edge of the meniscus on the substrate.<sup>19,31</sup> Due to water evaporation and lateral capillary forces (also referred to as capillary immersion forces<sup>23</sup>), the particles form a 2D array. The thickness of the 2D array depends on the angle between the plate and the water surface. The angle between the plate and the water surface can be controlled by the translation speed of the substrate and the height of the meniscus.

**Preparation: Mesoporous  $\text{TiO}_2$  Structure.** The detailed preparation process is shown schematically in Figure 2. Onto the  $\text{SiO}_2$  particle array was deposited 0.05 M titanyl acetylacetonate (Tokyo Kasei, Japan) in ethanol solution by a spray-pyrolysis technique at controlled temperatures.<sup>32</sup> During the pyrolysis, the titanyl acetylacetonate droplets were converted to  $\text{TiO}_2$ . The thicknesses of the  $\text{TiO}_2$  film overlayers as deposited on the  $\text{SiO}_2$  two-dimensional arrays were 1–2  $\mu\text{m}$ . Finally, the  $\text{TiO}_2$ – $\text{SiO}_2$  hybrid film was immobilized by attachment to a Ni sheet (Nilaco, Co., Japan) using epoxy, with the  $\text{TiO}_2$  layer facing the Ni, and the glass substrate was removed using 18% HF solution (Koso Chemical Co., Ltd., Japan). The HF solution dissolves the  $\text{SiO}_2$  but not the  $\text{TiO}_2$ , the epoxy, or the Ni substrate. In a previous paper,<sup>20</sup> we had not immobilized the film on the Ni sheet. In that case, when we flowed aqueous solution onto the mesostructured film sample, it broke up into small pieces, which then dispersed into the solution. To avoid this problem, we attached the  $\text{TiO}_2$  films onto the Ni substrate. The most important aspect of this technique, however, is the fact that we were able to repeat the dipping process into the  $\text{AgNO}_3$  solution, carry out repeated photodepositions, and then locate the same microscopic areas again with the scanning electron microscope (JSM-5400, JEOL Ltd., Japan). In this fashion, the progress of the photodeposition was monitored.

**Photodeposition of Ag.** The  $\text{TiO}_2$  films were placed in a 10 mM  $\text{AgNO}_3$  aqueous solution (with 10% ethanol) under UV irradiation (365 nm, 9.5 mW). To examine the photoreduction process in detail, we wanted to observe the manner in which the Ag particles were deposited onto the  $\text{TiO}_2$  mesostructures. Therefore, after an initial SEM observation, an Ag photodeposition was carried out, with the sample being subjected to irradiation for 5–30 min. The same precise locations on the film

(28) Knotek, M. L.; Feibelman, P. J. *Phys. Rev. Lett.* **1978**, *40*, 964.

(29) Wang, L.-Q.; Baer, D. R.; Engelhard, M. H. *Surf. Sci.* **1994**, *320*, 295.

(30) Wang, L.-Q.; Baer, D. R.; Engelhard, M. H.; Shultz, A. N. *Surf. Sci.* **1995**, *344*, 237.

(31) Denkov, N. D.; Veleev, O. D.; Kralchevsky, P. A.; Ivanov, I. B.; Yoshimura, H.; Nagayama, K. *Langmuir* **1992**, *8*, 3183.

(32) Sakai, H.; Baba, R.; Fujishima, A. *J. Electroanal. Chem.* **1994**, *379*, 199.

were examined using SEM after two such deposition procedures in order to examine the effect of irradiation time. For comparison, random areas of the irradiated films were also examined, that is, areas that had not previously been subjected to the high-intensity electron beam, to check for the possible effect of electron beam damage on the subsequent photocatalytic activity.

To estimate the percentage of Ag coverage on the  $\text{TiO}_2$  mesostructures, simple imaging analysis was carried out. The SEM images were first digitized. Next, the contrast was heightened so that the deposited Ag appeared white, and finally the percentage of this white area versus the total image area was estimated using image processing software (NIH Image).

### Results and Discussion

**Nanostructures.** We selected  $\text{SiO}_2$  particles for use in the preparation of the 2D ordered array replica templates, because they are commercially available in monodisperse form and are stable at  $\text{TiO}_2$  annealing temperatures (400–500 °C).  $\text{SiO}_2$  particles have one disadvantage, which is that they have a much different surface character (particularly the contact angle between the particles and the solvent) compared to those of other commonly used 2D array materials (e.g., latex and protein particles), and thus it is very difficult to prepare broad area (e.g., centimeter order)  $\text{SiO}_2$  2D arrays. At present, although we are not able to prepare such large arrays, we were, nevertheless, able to obtain millimeter-order samples (typically,  $2 \times 2 \text{ mm}^2$ ), which were large enough for convenient handling during the replication and microscopic examination.

Figure 3a shows an SEM image of an  $\text{SiO}_2$  ( $530 \pm 50 \text{ nm}$  diameter)– $\text{TiO}_2$  hybrid film, as observed from the silica particle side, after annealing at 450 °C. Even after the titanyl acetylacetonate mist was sprayed onto the  $\text{SiO}_2$  particle array, the particles maintained their array form. Figure 3b is an expanded image of Figure 3a. Figure 3c shows an SEM image of the surface after HF treatment of the sample shown in Figure 3a. Hollow spheres, with a bulblike morphology, were observed to have been formed in a closely packed regular array. Therefore, using the present procedure, we were able to obtain  $\text{TiO}_2$  films which were replicas of the  $\text{SiO}_2$  two-dimensional arrays.

The  $\text{TiO}_2$  film morphology was found to vary with the heating temperature (400–500 °C) used in the  $\text{TiO}_2$  spray-pyrolysis method. When the pyrolysis was carried out at 430 °C, instead of 450 °C, a different type of structure was observed (Figure 3d), with some cells exhibiting cuplike morphology. The side walls of these cells were thicker than those shown in Figure 3c. Needlelike structures can also be observed on the surface in the images (see arrows). These structures form as a result of the titanyl acetylacetonate solution soaking into the second and third layers of particles during the spray process, after removal of the silica particles.<sup>16</sup>

**Photodeposition of Ag.** If the preparation procedure for the mesostructured  $\text{TiO}_2$  films is successful, they should exhibit significant photocatalytic activity. We were concerned about the possibility of the OH groups being replaced by F on the  $\text{TiO}_2$  surface, which could degrade the photocatalytic activity,<sup>33</sup> and therefore, we examined the photocatalytic activity after the HF treatment. In general, to evaluate the photocatalytic activity of  $\text{TiO}_2$ , researchers measure the photodecomposition of organic materials. However, in the present work, we sought to selectively examine the photocatalytic activity of the textured side of the film. If the photodecomposition method were used, it would be difficult to distinguish whether the photoactivity was due to the textured side.

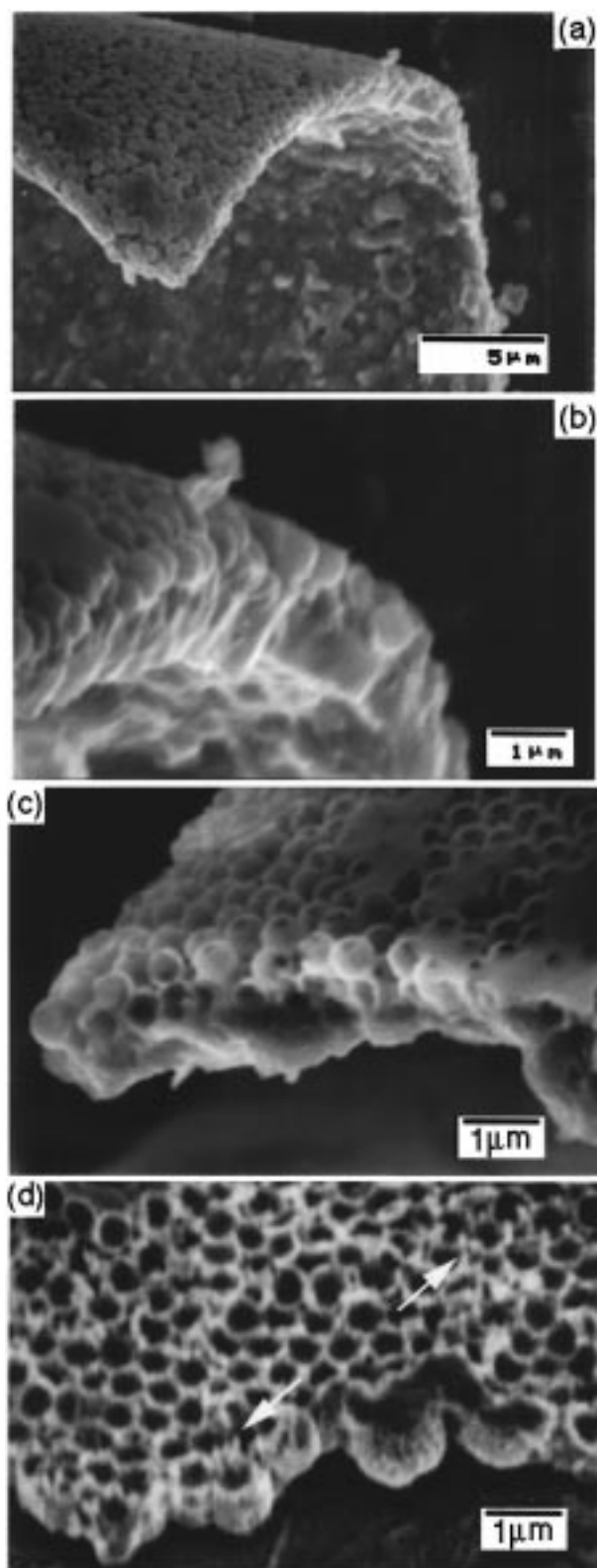


**Figure 3.** SEM image of a  $\text{SiO}_2$ – $\text{TiO}_2$  hybrid film (a) and Expanded image of a cross section of the hybrid film (b) and of replicated  $\text{TiO}_2$  films heated at (c) 450 and (d) 430 °C.

For this purpose, the photodeposition of Ag particles is a convenient, directly observable method, for example, using microscopy.<sup>26</sup>

After the  $\text{AgNO}_3$  photoreduction, we observed the localized reflection of light from silver particles on the mesotextured side of the  $\text{TiO}_2$  film by use of optical microscopy (not shown). The presence of metallic silver



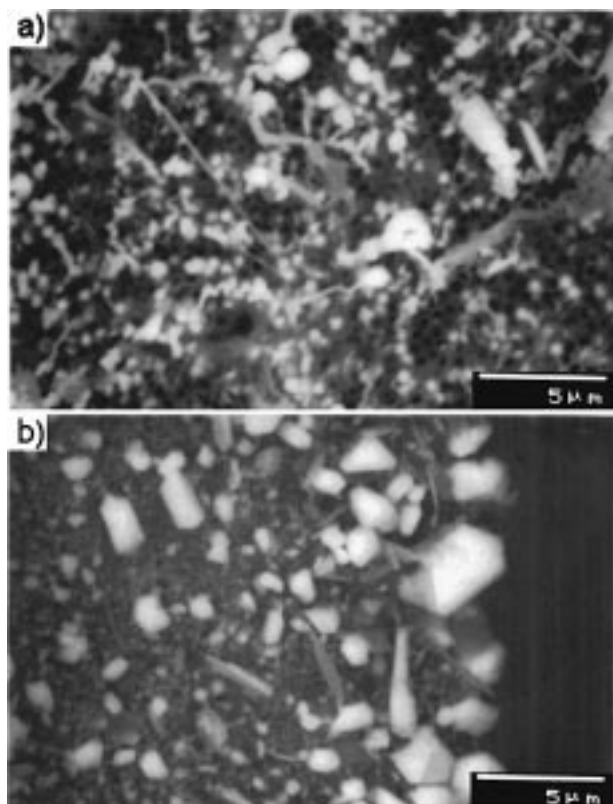


**Figure 4.** Backscattered electron images (BEIs) of the (a) bulblike and (b) cuplike structures after 15 min of photodeposition under UV irradiation.

indicates that the  $\text{TiO}_2$  was active for photoreduction. To examine the photoreduction process in more detail, we obtained images of the film after photodeposition using SEM in the backscattered electron imaging mode. In the backscattered electron image (BEI), high-electron-density atoms are observed as brighter than low-electron-density ones. Of the sample constituents ( $\text{TiO}_2$ ,  $\text{SiO}_2$ , Ag), Ag has the highest electron density. Therefore, if the mesoporous  $\text{TiO}_2$  surface has photocatalytic activity, we expect to observe bright areas due to Ag.

Figure 4 shows lower magnification BEIs of the bulb (panel a) and cuplike (panel b) structures after 15 min of photodeposition under UV irradiation. Ag particles covered about 40% of the surface in both cases (38.8% and 39.5% in a and b, respectively). Thus we can conclude that both mesoporous  $\text{TiO}_2$  structures have high photocatalytic activity even after HF treatment. Later, we will show, however, that there are subtle differences in the nucleation process on the two types of structures.

Herrmann et al.<sup>26</sup> have previously reported the photocatalytic deposition of silver on  $\text{TiO}_2$  powder. They examined the kinetics of silver deposition quantitatively by measuring the amounts of silver deposited. They reported, using a suspension of titanium dioxide powder (Degussa P-25, mainly anatase) in 0.1 M  $\text{AgNO}_3$ , that the mass of deposited metal per unit mass of Ti powder increases monotonically with irradiation time. In the present work, we also observed increasing deposition with UV irradiation time on the mesoporous  $\text{TiO}_2$  films. Figure 5a shows a BEI of the film before deposition. We can observe that this film has cuplike morphology. Figure 5b shows another, previously unexamined location (to avoid complications due to possible electron beam damage, as discussed later) on the same film after 5 min of photodeposition under UV irradiation. A large number of Ag particles (bright areas) can be observed on the surface.

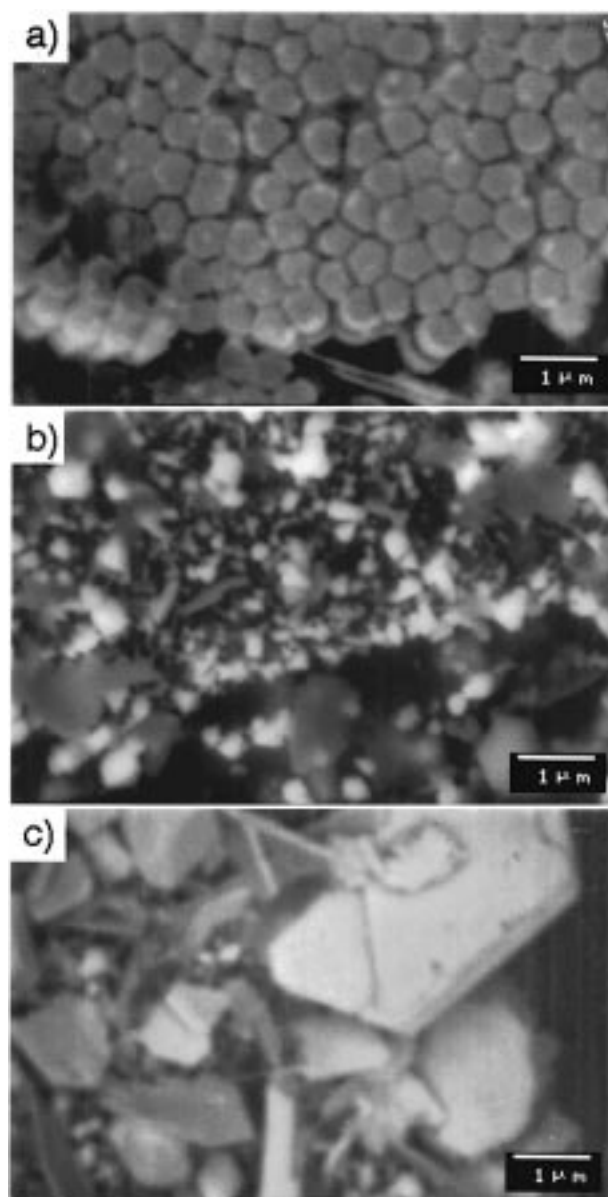


**Figure 5.** SEM images of replicated  $\text{TiO}_2$  films heated at 450 °C (backscattered electron images) at different locations: (a) before deposition; (b) after 5 min of photodeposition under UV irradiation, and (c) after an additional 25 min of photodeposition under UV irradiation (365 nm, 9.5 mW).

The range of particle sizes is from 0.01 to 1  $\mu\text{m}$ . In Figure 5c, again at a new location on the same film, we found that the average size of the bright areas ( $\sim 2 \mu\text{m}$ ) was larger after an additional 25 min of photodeposition. The presence of Ag was also confirmed using energy-dispersive X-ray analysis (EDX). It should also be noted that a small amount of Ni was observed, which could have been due either to the Ni substrate or to a trace of Ni being dissolved in the HF and then depositing on the  $\text{TiO}_2$  film surface.<sup>34</sup>

After confirming that the mesostructures have photocatalytic activity and that the amount of Ag deposited increases with time, we examined the effect of irradiation time at specific microscopic locations. This type of repeat observation was made possible by the immobilization process (see Materials and Methods). We examined the same location of the same film after various lengths of irradiation time (2–30 min) by use of SEM in both the

(34) Matsushita, S. I.; Miwa, T.; Tryk, D. A.; Fujishima, A. Manuscript in preparation.

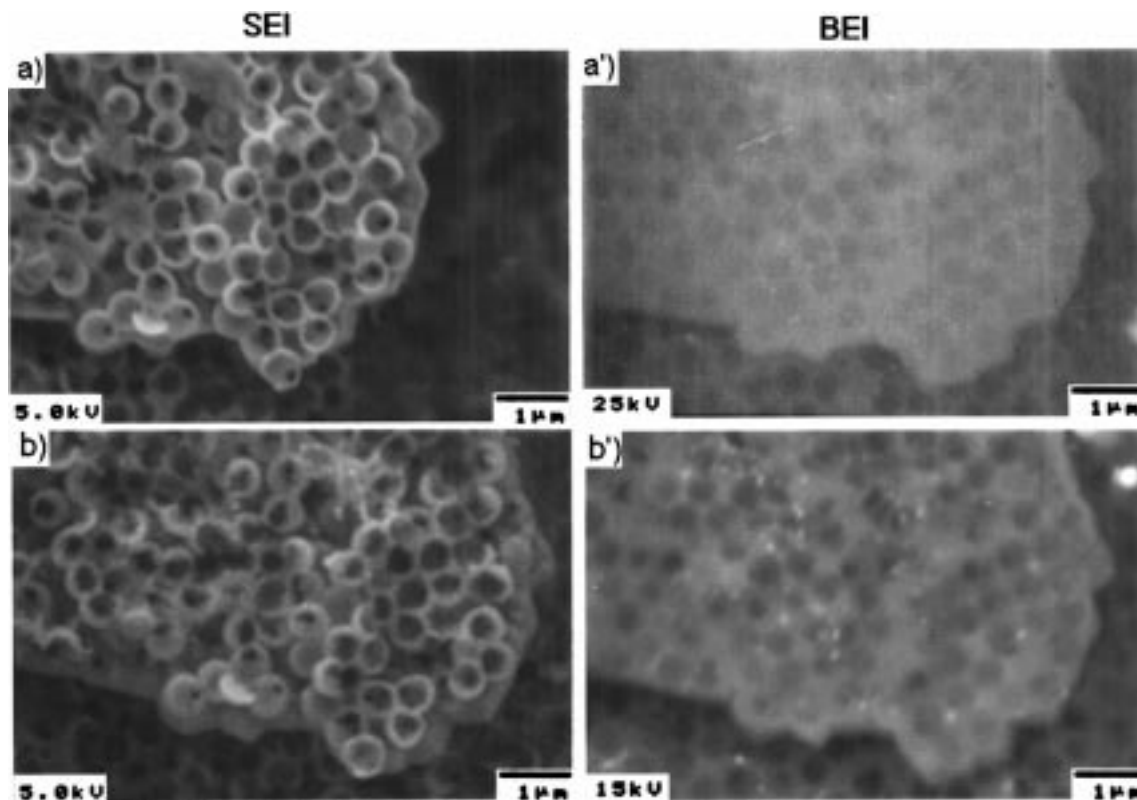


**Figure 6.** SEM images of replicated TiO<sub>2</sub> films heated at 450 °C (secondary electron images (SEIs) and backscattered electron images (BEIs)) at specific locations: (a and a') before deposition and (b and b') after 5 min of photodeposition under UV irradiation (365 nm, 9.5 mW). Previous to this, we had also carried out one SEM observation after 2 min of photodeposition (not shown).

secondary electron imaging and BEI modes. In the secondary electron images (SEIs), we confirmed that some material deposited on the thin walls of the bulblike pores after the photodeposition (comparing parts a and b of Figure 6). In the BEI obtained after photodeposition (Figure 6b'), we observed small dots, on the order of tens of nanometers, with high backscattering intensity after the photodeposition. The distribution of the dots, which were also observed in the SEI (Figure 6b), was correlated with high BE intensity (Figure 6b'). Therefore, we conclude that these small dots are due to photodeposited Ag. However, the amount of deposited Ag in Figure 6b is much smaller than that in Figure 5b, even though the UV irradiation times were the same (5 min). The average size of the deposited Ag particles in Figure 6b is only 0.1  $\mu\text{m}$ , much less than that in Figure 5b (1  $\mu\text{m}$ ).

The reason for this apparent difference in photocatalytic activity was found to be that the SEM observation itself, that is, electron beam damage, was responsible for the decrease in activity. Figure 7 shows an extreme example, at lower magnification, of the effect of the electron beam. A large amount of Ag was deposited outside the circular area in the center of the image, but little was deposited inside this area. Prior to the photodeposition, we had examined this small area with SEM (acceleration voltage, 15 kV). Subsequently, the Ag photodeposition was carried out for 15 min. It is clear that the electron beam-exposed area was much less active for Ag photodeposition.

The fact that electron beam exposure can create defects on TiO<sub>2</sub> surfaces is relatively well-known.<sup>30,35–38</sup> Such defects could be expected to create energy states within

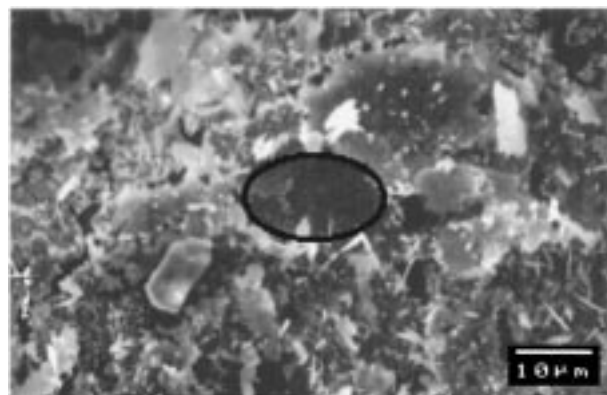


**Figure 7.** SEM image of an Ag-deposited porous TiO<sub>2</sub> film that had been annealed prior to the photodeposition. A high-energy beam (acceleration voltage, 15 kV) was focused on the circular area prior to the deposition. The photodeposition was carried out under UV irradiation (365 nm, 9.5 mW) for 15 min.

the band gap, leading to enhanced recombination.<sup>39</sup> Therefore, it is not surprising that the photocatalytic activity would be impaired.

**Effect of Cell Structure.** The use of Ag photodeposition as a means of monitoring photocatalytic activity allows us to examine directly the influence of the detailed morphology (cup vs bulb) of the meso-structured films. As already shown, the overall amount of Ag deposited was little affected by the morphology. However, the nucleation process was found to differ in a subtle manner. Figure 8 shows expanded SEIs of the replicated TiO<sub>2</sub> films after Ag photodeposition (annealed at 450 and 430 °C; UV irradiation time, 15 min). We were able to obtain

(35) Patel, R.; Guo, Q.; Cocks, I.; Williams, E. M.; Roman, E.; Segovia, J. L. *J. Vac. Sci. Technol., A* **1997**, *15*, 2553.

(36) Eriksen, S.; Egdell, R. G. *Surf. Sci.* **1987**, *180*, 263.

(37) Sham, T. K.; Lazarus, M. S. *Chem. Phys. Lett.* **1979**, *68*, 426.

(38) Lazarus, M. S.; Sham, T. K. *Chem. Phys. Lett.* **1982**, *92*, 670.

(39) Sze, S. M. *Physics of Semiconductor Devices*; John Wiley & Sons: New York, 1981.

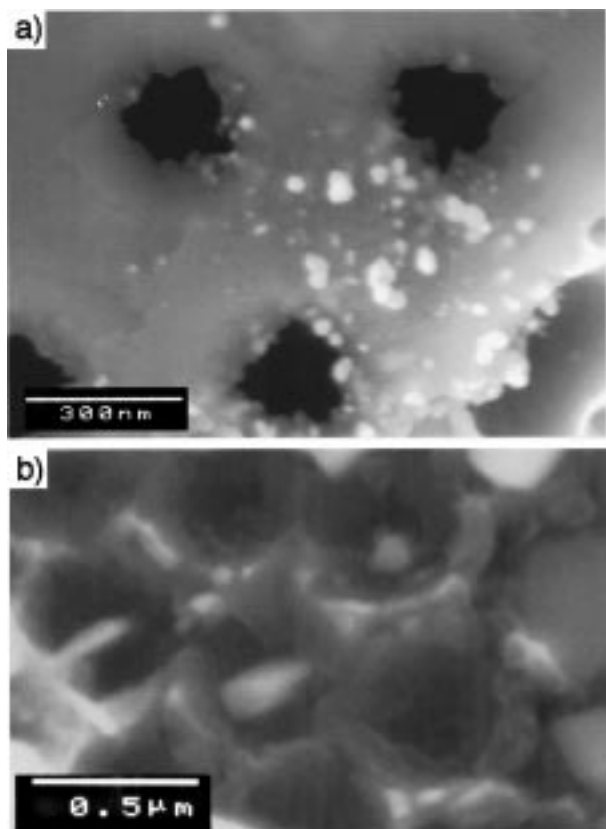


**Figure 8.** Expanded SEM images of Ag-deposited porous TiO<sub>2</sub> films heated at (a) 450 and (b) 430 °C.

information concerning the wall edges of the meso-ordered cells in both the films prepared at 430 °C (Figure 8a) and also those prepared at 450 °C (Figure 8b). The wall edges of the films prepared at 430 °C have rectangular corners, whereas those of the films prepared at 450 °C have sharp, knifelike edges.

In the case of the films heated at 450 °C, with bulblike structures, the Ag photodeposition was not specifically localized on any particular part of the microtextured surface (Figure 8a). However, for the films heated at 430 °C, which were characterized by cuplike structures, the Ag deposits were observed at the bottoms of the cups as distinct particles and as strips along the rims of these structures (Figure 8b). One possible reason is the distribution of the light flux at the surface. However, the light is able to pass through the very thin (10 nm) wall. Therefore, the differences in the Ag deposition most likely did not result from differences in the light flux distribution.

The most likely cause of the difference in behavior involves the wall thickness. Generally, the walls of the films heated at 430 °C are thicker (greater than ~10 nm) than those of films heated at 450 °C (less than ~5 nm). The electron mobility and lifetime may depend on the wall thickness. When the wall is relatively thin, the recombination of photogenerated electrons and holes is expected to be relatively small, with the electrons being efficiently trapped at the surface.<sup>40</sup> Accordingly, the reduction sites should be dispersed over the entire area of the thinner wall (Figure 9a). This is in contrast to the case with the thicker wall (see below).

As discussed above for the cuplike structures, the Ag deposition could be observed in two areas (Figure 9b), that is, at the cup bottoms and along the rims of these

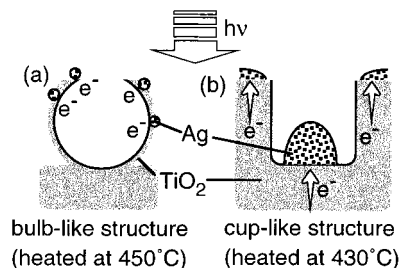


**Figure 9.** Schematic model for the photocatalytic deposition of Ag in the mesostructured porous TiO<sub>2</sub> films heated at (a) 450 °C (bulblike structures) and (b) 430 °C (cuplike structures).

structures. Considering the possible reasons for the Ag deposition on the bottoms of the cups, the deposition process may involve the influence of the bulk TiO<sub>2</sub> underlying the periodic structures. UV light excites the electron–hole pairs in this bulk TiO<sub>2</sub>, and the excited electrons then find the shortest path to the surface, that is, to the bottoms of the cups. After Ag nuclei are deposited at these points, electrons tend to be channeled to these sites because of the very low overpotential for Ag deposition on the Ag metal surface.<sup>41</sup> As a result, the Ag deposits grew into pillar shapes in the cuplike structures. In the case of the top edges of the cups, the same type of geometric argument can be used as that involved for the thin wall situation. In other words, electrons that are photogenerated near the edge have relatively good access to the surface, at which they can first be trapped at defect sites and then react with Ag<sup>+</sup>.<sup>42</sup>

### Summary and Conclusions

TiO<sub>2</sub> films with hexagonally arrayed mesopores were prepared via a replication technique from two-dimensionally ordered arrays of monodisperse SiO<sub>2</sub> particles (~530 nm). In very recent work, we have also found that the pore sizes can be controlled by varying the diameters of the silica particles over the range from 0.1 to 1.0 μm.<sup>17</sup> In addition, using latex particles, we have found it possible to form thin films with ordered pore structures directly on the substrate of interest.<sup>18</sup> In the work presented here, we found that the pore structures in the films depended sensitively on the annealing temperature, the major difference being the thickness of the pore walls. The thinner walled (bulblike) structures were formed at 450 °C, whereas the thicker-walled (cuplike) structures were formed at 430 °C.

These TiO<sub>2</sub> mesostructures exhibited photocatalytic activity, as evidenced by the photoreduction of Ag<sup>+</sup> to produce metal particles even after it was exposed to aqueous HF. We examined the progress of the photodeposition of Ag particles by use of optical microscopy and scanning electron microscopy, with both secondary electron and backscattered electron detection. The activities were essentially the same for the bulblike and cuplike morphologies. The amount of deposited silver increased with irradiation time.

The use of a rigid macroscopic support (Ni) enabled us to perform microscopic examination (SEM) at specific locations, carry out the photodeposition, and then find the same location again with SEM. However, the repeated exposure of the same location to the high-energy electron beam during the SEM observation was found to degrade the photocatalytic activity.

(40) Rothenberger, G.; Moser, J.; Grätzel, M.; Serpone, N.; Sharma, D. K. *J. Am. Chem. Soc.* **1985**, *107*, 8054.

(41) Wang, C.-M.; Heller, A.; Gerischer, H. *J. Am. Chem. Soc.* **1992**, *114*, 5230.

(42) Gerischer, H.; Heller, A. *J. Phys. Chem.* **1991**, *95*, 5261.



This was concluded on the basis of comparison of the photodeposition on areas that had previously been exposed to a highly focused electron beam with that on areas that had not been. The detailed nature of the nucleation process for Ag photodeposition was found to depend on the pore morphology. In the case of the thin-walled bulblike structures, Ag nanoparticles deposited randomly, because the photogenerated electrons that are generated within the walls are quickly trapped at the wall surface. In the case of the cuplike structures, photogenerated electrons from the bulk first reach the cup bottoms and nucleate particles therein.

On the basis of the present results, the 2D particle array template technique appears to offer a viable approach to the highly controlled preparation of ordered mesoporous photocatalytic  $\text{TiO}_2$  films.

**Acknowledgment.** Thanks are due to Professor K. Hashimoto (Research Center for Advanced Science and Technology, University of Tokyo, Japan) and Professor T. E. Mallouk (The Pennsylvania State University) for their valuable discussions and to Dr. A. S. Dimitrov (L'OREAL Tsukuba Center, Japan) for development of the glass cell used in the preparation of the particle coatings and to Mr. N. Sakai and Mr. Y. Kawato (University of Tokyo, Japan) for their valuable assistance. The present work has been partially supported by a Grant-in-Aid for Scientific Research from the Ministry of Education, Science, Sport and Culture of Japan, by the YKK R & D Center, and by the Circle for the Promotion of Science and Engineering.

LA981106Z